



Published in final edited form as:

IEEE Trans Rehabil Eng. 1998 March ; 6(1): 75–87.

Robot-Aided Neurorehabilitation

Hermano Igo Krebs [Member, IEEE],

Mechanical Engineering Department, Newman Laboratory for Biomechanics and Human Rehabilitation, Massachusetts Institute of Technology, Cambridge, MA 02139 USA (e-mail: hikrebs@mit.edu).

Neville Hogan,

Mechanical Engineering Department, Newman Laboratory for Biomechanics and Human Rehabilitation, and Brain and Cognitive Sciences Department, the Massachusetts Institute of Technology, Cambridge, MA 02139 USA (e-mail: neville@mit.edu).

Mindy L. Aisen, and

Department of Neurology and Neuroscience, Burke Institute of Medical Research, Cornell University Medical College, White Plains, NY 14850 USA (e-mail: volpe@rockvax.rockefeller.edu).

Bruce T. Volpe

Department of Neurology and Neuroscience, Burke Institute of Medical Research, Cornell University Medical College, White Plains, NY 14850 USA (e-mail: volpe@rockvax.rockefeller.edu).

Abstract

Our goal is to apply robotics and automation technology to assist, enhance, quantify, and document neurorehabilitation. This paper reviews a clinical trial involving 20 stroke patients with a prototype robot-aided rehabilitation facility developed at the Massachusetts Institute of Technology, Cambridge, (MIT) and tested at Burke Rehabilitation Hospital, White Plains, NY. It also presents our approach to analyze kinematic data collected in the robot-aided assessment procedure. In particular, we present evidence 1) that robot-aided therapy does not have adverse effects, 2) that patients tolerate the procedure, and 3) that peripheral manipulation of the impaired limb may influence brain recovery. These results are based on standard clinical assessment procedures. We also present one approach using kinematic data in a robot-aided assessment procedure.

I. INTRODUCTION

THE leading cause of permanent disability in the United States is cerebral vascular accident, namely: stroke. According to figures from the National Stroke Association (NSA), in 1993 there were 550 000 patients with stroke in the United States. The consequences were devastating, 150 000 died (the third leading cause of death), and there were 350 000 disabled survivors. The estimated cost of care was \$30 billion. Graying of the population will almost certainly aggravate this problem, since the relative incidence of stroke doubles for every decade after 55 years old, and the leading edge of the baby-boom will shortly reach age 55. The neurorehabilitation process is laborintensive, relying on therapy and evaluation procedures that

Copyright © 1998 IEEE.

Reprinted from IEEE Transactions on Rehabilitation Engineering.

This material is posted here with permission of the IEEE. Such permission of the IEEE does not in any way imply IEEE endorsement of any of this web site's products or services. Internal or personal use of this material is permitted. However, permission to reprint/republish this material for advertising or promotional purposes or for creating new collective works for resale or redistribution must be obtained from the IEEE by writing to pubs-permissions@ieee.org.

By choosing to view this document, you agree to all provisions of the copyright laws protecting it.

are administered by a clinician working with a single patient. This one-on-one interaction characterizes much of the practice of clinical neurology. Labor-intensive procedures are a primary application field for robotics. Indeed in clinical neurology, our research suggests that robotics and information technology may be used to improve quality, enhance documentation, increase productivity and reduce cost. However, whether exercising the patients' paralyzed limbs has a positive effect on neurological restoration of function remains controversial. In short, the kind of assistance a robot could provide might not matter.

Several studies have reported positive outcomes with different approaches, including repetitive passive exercises [1], forced use of the paretic limb by restraining the contralateral limb [2], [3] increased amounts of therapy and external manipulation [4], [5] biofeedback [6], and functional electrical stimulation [7]. Nevertheless, the efficacy of these different therapy techniques remains controversial. In fact, studies examining differences in outcomes between techniques showed little variation or none [8], [9]. On a more mechanistic level, stroke recovery is only partially understood with two main assumptions encompassing the recovery process. One assumption is that parallel brain regions in the unaffected hemisphere take on functions of the contralateral hemisphere necrotic tissue, sending its commands via uncrossed pathways, i.e., not all descending brain fibers from one brain hemisphere cross over to the contralateral body hemisphere [10], [11]. The other assumption is that adjacent areas of undamaged brain tissue in the same hemisphere reorganize, taking on functions of the necrotic tissue. The reorganization of cortical maps has been demonstrated in the motor [12], sensory [13], [14], visual [15], and auditory maps [16]. Furthermore, recent animal studies have shown that the degree of reorganization of the remaining undamaged cortex in primates can be influenced by environment [17]. This result suggests that exercising the patients' paralyzed limbs might have a genuinely positive effect on neurological restoration of the limb function. The clinical trial described in this paper aimed to assess whether: a) robot-aided therapy has adverse effects, b) patients were tolerant of the procedure, and c) whether manipulation of the impaired limb influences motor recovery [18]. At the same time, this clinical trial provided quantitative data with which we could develop better tools to evaluate and understand the mechanism of recovery.

II. METHODS

A. Apparatus

MIT-MANUS is a novel robot designed for clinical neurological applications [19]. Unlike most industrial robots, MIT-MANUS is configured for safe, stable and compliant operation in close physical contact with humans. This is achieved using impedance control, a key feature of the robot control system [20]. Its computer control system modulates the way the robot reacts to mechanical perturbation from a patient or clinician and ensures a gentle compliant behavior. MIT-MANUS can move, guide or perturb the movement of a subject's or patient's upper limb and can record motions and mechanical quantities such as the position, velocity, and forces applied. The present design is portable and meets or exceeds applicable safety standards for operation in a clinical environment. The machine was designed to have a low intrinsic end-point impedance (i.e., be back-driveable), with a low and nearly-isotropic inertia (1 ± 0.33 kg, maximum anisotropy 2:1) and friction (0.84 ± 0.28 N, maximum anisotropy 2:1), and be capable of producing a predetermined range of forces (0–45 N) and impedances (0–2N/mm).

Furthermore, weight, visibility and accessibility to the patient's hand were key requirements. MIT-MANUS presently has two modules. A planar module provides two translational degrees of freedom (dof) for elbow and forearm motion [Fig. 1(a) and (b)]. It also permits a small range of passive vertical motion through a set of springs. A 3-dof module mounts on the end of the planar module and provides three degrees of freedom for wrist motion [Fig. 1(a) and (d)]. The 2-dof module is portable (390 N) and consists of a direct-drive five bar-linkage SCARA

(selective compliance assembly robot arm) mechanism driven by brushless motors rated to 7.86 Nm of continuous stall torque with 16-bit resolvers for position and velocity measurements. Redundant velocity sensing is provided by dc-tachometers with a sensitivity of 1.75 V/rad/s. Torque sensors on the motor shafts are rated to 22.6 Nm with a torsional stiffness of 2302 Nm/rad. To minimize noncollocation effects, actuators and sensors are aligned on the same axis. The resolvers and torque sensors are mounted on the brushless motor shaft outputs, while the tachometers are mounted on the motor shaft tips. The mechanism is mounted on a tubular base that allows its vertical position to be adjusted. The 3-dof module consists of a differential mechanism mounted on a parallelogram linkage driven by three geared actuators. The geared actuators are rated to a peak torque of 0.108 Nm. Position sensing is provided by built-in precision potentiometers with 0.9 Kohm/rad. The actuators include tachometers with a rated 0.07 V/rad/sec sensitivity. The robot control architecture is implemented in a standard personal computer (486 CPU—66 MHz) with 16-bit A/D and D/A I/O cards, as well as a DIO card with 32 digital lines. Besides its primary control function, this computer displays the exercise to be performed to both the operator and the subject or patient via a video-splitter with dedicated monitors. The neurorehabilitation workstation includes a second personal computer (386 CPU—25 MHz) for display of on-line video and audio information to the subject/patient. Communication between computers is achieved via a serial port at transmission rates that allow video update rates above 30 frames/s. The workstation is mounted on a custom-made adjustable table and chair, which allows the chair to be rotated 360° and translated 0.5 m toward a table-top, specially designed to facilitate transfer of wheelchair-bound patients. The chair includes three seat-belts to limit torso movements and an adjustable foot rest. The table-top can be translated 0.25 m vertically and was designed to allow continuous support of a patient/subject's elbow. The table-top surface is impregnated with Teflon and the elbow support base is made out of Teflon. Custom-made hand-holders were manufactured for the 3-dof and 2-dof modules. A 3-dof hand-holder latches through a magnetic lock, allowing quick connection and disconnection, while a custom-made hand-holder for the 2-dof module connects the subject/patient's impaired limb to the robot end-effector. Hand-holders [Fig. 1(c)] were manufactured for both arms and in different sizes out of high-density polyethylene or braided carbon-fiber and marine based epoxy resin.

B. Subjects

Consecutive patients ($N = 20$) with a single stroke and hemiparesis caused by a CT-verified cerebral vascular accident in the cortical or subcortical motor area served as subjects for the study, in accordance with the guidelines and approval of the MIT Committee on the Use of Humans as Experimental Subjects and Burke Rehabilitation Hospital Human Subject Committee. Written consent was obtained from all subjects or designated guardians. A detailed description of patients characteristics, i.e., sex, age, affected limb, lesion location, type, and size, assessment scores, and complications, can be found in Aisen [18].

C. Experimental Procedure

In this clinical trial with twenty sequential hemiparetic patients, only the 2-dof module was used. The staggered pool of twenty patients were admitted to the same hospital ward at Burke Rehabilitation Hospital and assigned to the same team of rehabilitation professionals.¹ They were enrolled in either a robot-aided therapy group (RT, $N = 10$) or in a group receiving standard therapy plus “sham” robot-aided therapy (ST, $N = 10$). Both groups were comparable in age,

¹Recruited patients were automatically enrolled in the experimental or control group based on the criterion that at any time there would be no more than three patients in the experimental group. If at the time of admission to the study, the experimental group had less than three patients, the patient was assigned to the experimental group. If at the time of admission to the study, the experimental group had three patients, the patient was assigned to the control group. When the experimental group reached the goal size of 10, all the remaining patients were assigned to the control group until it also reached the same goal size.

physical impairment, and time between onset of the stroke and admission to the rehabilitation hospital (mean age: RT 58.5, ST 63; mean admission to rehabilitation in weeks since stroke onset: RT 2.8, ST 3.2). All patients were blinded to the treatment group and were assigned to the same blinded clinical team (double blind study). Both groups received conventional therapy; the RT group received an additional 4–5 h/week of robot-aided therapy consisting of peripheral manipulation of the impaired limb correlated with audio-visual stimuli, while the ST group had an hour of weekly robot exposure.

The sensory-motor motor training for the RT group consisted of a set of “video-games.” Patients were required to move the robot end-effector according to the game’s goals. If the patient could not perform the task in response to a visual and auditory cue, the robot assisted and guided the patient’s hand. Menu-driven software allowed the clinician to choose different values of impedance (very soft, soft, medium, hard, very hard). However, we opted to use the same soft range (100 N/m, 2 N-s/m) throughout this trial primarily due to patients’ pretrial preferences and also to minimize any risk of exacerbating joint or tendon pain. For this trial, the impedance controller was implemented using nonlinear position and velocity feedback structured to produce a constant isotropic end-point stiffness and damping. Coupled to our highly back-driveable design, the stability of this controller is extremely robust to the uncertainties due to physical contact [21], [22]. The impedance controller implementation was as follows:

$$\tau = -J^T(q) \cdot [K_p \tilde{x} + K_D \dot{\tilde{x}}] \quad (1)$$

where τ is the joint torques, $J(q)$ is the manipulator Jacobian, q is a vector of joint angles, $\tilde{x} = x - x_{\text{desired}}$ is a vector of displacement from a nominally desired position, K_p is the stiffness matrix in N/m, and K_D is the damping matrix in N-s/m, with

$$K_p = \begin{bmatrix} 100 & 0 \\ 0 & 100 \end{bmatrix} \quad K_D = \begin{bmatrix} 2 & 0 \\ 0 & 2 \end{bmatrix}.$$

The games were designed to evaluate the stroke patient’s recovery of upper-limb motor function and to document and characterize stroke recovery in all of its phases. The games included drawing circles, stars, squares, diamonds, and navigating through “windows,” as illustrated in Fig. 2(a) and (b). Some games required predominantly shoulder motion, while others required predominantly elbow motion. Additional games required the coordination of both shoulder and elbow. The games were designed to maximize correlated sensory feedback, including visual, audio, and proprioceptive sensory stimuli; to be visually evoked and visually guided; and to occupy the same workspace.

The procedure typically lasted for about seven weeks, and consisted of a daily exercise with the normal limb followed by three packets of 20 repetitions of the daily exercise with the impaired limb (robot-guided). Each packet was preceded and succeeded by an active (patient-guided) or manually guided exercise (clinician-guided). Typical cumulative numbers for a seven week program were 25 sessions with 1500 repetitions of a game, 100 nonassisted repetitions, and three evaluation sessions.

The training for the ST group was similar to the RT group, except that half of the one hour session consisted of playing the video games with the unimpaired arm and half the session with the impaired arm while the robot passively supported the arm and provided the video-game visual feedback (position feedback). If the patient could not perform the task, he/she used the unimpaired arm to assist and complete the game (self-ranging), or the clinician assisted.

A standard assessment procedure was used every other week to assess all patients (robot-aided therapy group and control group). The standard assessment was always performed by the same rehabilitation professional for all the patients involved in the study. This professional was not directly involved with the robot-aided therapy and did not know who was enrolled in the experimental group or control group. The standard assessment procedure used widely accepted procedures including: functional independence measure (FIM) and the upper limb subsection of the Fugl–Meyer (F–M) scales [23], [24]. FIM is an adequate scale to measure competence in completing functional tasks, such as dressing. However, its score does not depend solely on motor control, but also on intangible factors such as patient’s personality, depression state, and dependent attitude. The Fugl–Meyer is a scale that measures motor impairment. The pitfalls of relying on the upper limb subsection of the Fugl–Meyer in our trial were that most patients were transferred to the acute rehabilitation hospital three weeks after the onset of the stroke. Therefore, the Fugl–Meyer scale could potentially suffer from a decrease in resolution, since the return of reflex and synergistic movements, which represent a substantial component of the total score, might have taken place before the patients were admitted to the rehabilitation hospital. Instead of a broad range with end-of-scale values of 66 for the upper extremity, a potential range of six points for isolated shoulder and elbow movement was expected. To increase the number of isolated muscle groups assessed in the paretic limb, a scale based on the Fugl–Meyer approach, the upper extremity motor status score (MSS), was used [18]. Likewise to assess strength in the biceps, triceps, anterior and lateral deltoid muscles, the standard assessment procedure included a scale validated in other clinical trials: the motor power scale (MP) [25].

D. Robot-Aided Assessment Procedure: Quantization of Kinematics

The standard assessment procedures listed above are human-administered, which may mitigate their reliability and effectiveness. Instrumentation on board the robot records kinematic and force data that may permit new assessment procedures with improved objectivity, repeatability, precision and ease of application. Robot-aided assessment procedures may also provide new insight into the process of recovery. In this paper, only an analysis of the kinematic profile of the movement of patients is presented. This component of the robot-aided assessment procedure is based on a century old conjecture in motor neuroscience—Woodworth, 1899 [26]. This conjecture suggests that human arm movement is composed of a sequence of submovements. Woodworth argued that movement is composed of two sorts of submovement components: the initial impulse and the “current” control. The “current” control consisted of a sequence of finer adjustments added to the initial impulse as the hand approached the target. He argued that “current” control could be eliminated by either having the person close his eyes or by requiring very fast movements. Several variants of this idea have been proposed many times in the motor neuroscience literature. For example, Crossman and Goodeve proposed that a periodic single shape, scaled and dilated, could describe movement segments. They considered periodic submovements with displacement profiles in the shape of an error function (erf) [27]. Morasso and Mussa-Ivaldi considered periodic submovements, which they called “strokes” to describe trajectory formation and handwriting. They used B-Splines to represent velocity submovements [28]. Jagacinski showed that the periodicity in the submovement models was unacceptable [29], [30]. The striking character of our data (see Fig. 5, discussed later) led us to postulate that a repertoire of movement primitives, each with a bell-shaped velocity profile, constitute the building blocks of complex tasks. Evidence of submovements is illustrated in Fig. 3(a) which shows a typical set of circles drawn by a neurologically normal subject. The left column shows the displacement of the hand in the plane, where X and Y are indicated in the figure sketch, and the right column shows the tangential speed. The instructions were to draw circles of approximately the size of a 0.25 m diameter ring at a constant speed. After drawing four circles, the normal subject was requested to redraw the circles faster. Fig. 3(b) shows a polar plot with the speed proportional to radius plotted versus displacement angle

around a center located at the mean value of x and y displacements for the five trials of Fig. 3 (a). The speed profiles were normalized to the maximum speed of the set and the initial accelerating and final decelerating regions are not shown. This plot reveals a remarkably consistent pattern and suggests a kinematic, not temporal, characteristic of the speed profile, and that the movement is composed of a small number of blended segments [31], [32]. We propose as a working hypothesis that this kind of “quantization” is a basic feature of human motor behavior, and used this hypothesis to develop a robot-aided assessment procedure.

The submovement concept can be expressed via the following synthesis equation:

$$f(x) = \sum_{i=1}^N c_i \cdot \Phi \left(\frac{x - b_i}{a_i} \right) \quad (2)$$

where f represents the signal, x is the independent variable, a_i, b_i, c_i are respectively, the dilation, translation, and modulation coefficients of the i -basis function, Φ is the basis function. In other words, we want to reconstruct $f(x)$ by modulating, by translating, and by dilating a “mother” shape (basis function). An unsupervised data analysis algorithm was designed to extract these postulated “quanta” from the experimental speed record. It is a “greedy” breadth-first search type algorithm called “irregular sampling radial basis function algorithm” (ISRBF) [31]; modulating, translating, and dilating a “mother” shape to fit the symmetric region of the speed profile peaks. The “mother” shape was experimentally determined, and it resembles the minimum-jerk speed profile of a point-to-point movement. The algorithm consists of a pyramidal decomposition scheme to design the scattered center radial basis network illustrated in Fig. 4. At each pass, the maximum speed peak and adjacent symmetric region is fitted in a least-squares sense with a radial basis function. The fitted basis function is subtracted from the data stream, and the remainder is iterated through the algorithm. This pyramidal decomposition method suffices in guaranteeing fidelity of reproduction for a sufficiently large number of scattered centers with the process ending when the remainder is within a predetermined precision bound. However, the objective is to decompose the human arm movement into segments or submovements. Unfortunately, not all speed peaks necessarily correspond to segments. Movement curvature was used to bound the maximum number of submovements or centers (Cn). Curvature can be described by

$$K(t) = \partial\theta/\partial s \quad (3)$$

where θ is the instantaneous velocity angle (in the horizontal plane $\arctan\left(\frac{v_x}{v_y}\right)$) and s is the displacement. This formulation is equivalent to the Frenet Formula

$$K(t) = \left[(\vec{v} \cdot \vec{v})(\vec{a} \cdot \vec{a}) - (\vec{v} \cdot \vec{a})^2 \right]^{\frac{1}{2}} / (\vec{v} \cdot \vec{v})^{\frac{3}{2}} \quad (4)$$

with v and a representing the first and second derivative, i.e. velocity and acceleration vectors of the curve $r(t)$, and the multiplication symbol represents a dot product. Viviani and Terzuolo showed the correlation between speed and the radius of curvature of human movements [33]; there is a corresponding peak in curvature for each dip in speed. This curvature trait is exploited to determine the maximum number of submovements or centers (Cn), i.e., the number of scattered center radial bases is limited to the number of peaks in curvature, and the pyramidal decoding algorithm terminates when the remainder is within a predetermined precision bound or the number of scattered centers reaches the predetermined maximum center number (Cn).

Furthermore, in this particular application, any basis function with duration under 100 ms was eliminated from the approximation function, as we expect arm submovements to last longer. Since the curvature has a peak when the speed is close to zero, a perfectly straight point-to-point movement (one submovement) has an infinite peak at the beginning and at the end of this movement (two peaks). To account for these edge peaks, the unsupervised algorithm does not count any curvature peak occurring at the edges or outside the speed envelope (the curvature is kept zero outside the speed envelope), but adds one to the determined total number of peaks. The beginning and the end of a movement (speed envelope) are determined when the speed record surpasses 1% of the maximum speed peak or falls under this threshold. To account for noise any curvature peak under 5% of the maximum curvature peak is not considered. The pyramidal decoder was originally used as an initial search vector for a radial basis network with movable centers called generalized radial basis function (GRBF) by Poggio and Girosi [34]. The GRBF attempts to solve the regularization problem with fidelity of reproduction and smoothness, while addressing the requirement to reduce the number of network units. This heuristic approach converges to a local minimum allowing translation and modulation of the bases, but no dilation. This approach did not show any substantial improvement in the decomposition (in the L2-sense), and added computational time. Therefore, the ISRBF algorithm used in the robot-aided assessment procedure retains only the pyramidal decoder component.

III. RESULTS

At the outset it was unclear whether robot-aided therapy would not impede recovery or exacerbate joint or tendon pain. In general close to 30% of stroke patients develop pain. Therefore, we had to address the potentially unsalvageable possibility of the robot-aided procedure having detrimental effects. The standard assessment procedure included the assessment of pain in joint or tendon for shoulder, wrist, and hand, as well as shoulder-hand syndrome. The results were reassuring: there was no difference between groups with seven controls and five experimental subjects developing pain in joints or tendons, and of these, three controls, and four experimental subjects developed shoulder-hand syndrome [18]. Furthermore, no adverse events occurred in an estimated 500 h of operation in close contact with patients. A questionnaire administered during the biweekly standard assessment by the therapists showed that robot-assisted therapy was well accepted and tolerated by the patients. The average questionnaire result for the patients is summarized in Table I. The last question was included specifically to assess the credibility of the questionnaire results, since a preference for the robot over a human therapist was considered extremely improbable. To minimize any influence in the standard therapy and evaluation, therapists were kept blind to the robot-aided therapy procedure (see Experimental Procedure). Therefore, we can not evaluate staff response to the robot-aided therapy. A detailed study of staff acceptance with an analog robotic device can be found elsewhere [35].

Results indicated that patients in the experimental group improved further and faster, outranking the control group in all the clinical assessments of the motor impairment involving shoulder and elbow, as summarized in Table II. There is a clear trend in the Fugl-Meyer (F-M) and motor power (MP) scores favoring the experimental group ($p \leq 0.20$ and $p \leq 0.10$, one-tail t -test), and a statistically significant improvement in the Motor Status Score (MSS) for shoulder/elbow ($p < 0.05$, one-tail t -test) [18]. Indeed, the degree of improvement in accuracy and degree of voluntary isolated movement in the specific muscle groups trained by the robot as reflected by the MSS for shoulder/elbow is striking. Although not achieving statistical significance, the Fugl-Meyer and MP scores suggest a distinguishable trend for greater improvement in the experimental group than the control group. The potential for generalization of the exercise therapy effect to other segments of the arm not exercised during the procedure were evaluated via the MSS scores for wrist and hand. Notwithstanding the observable trend

for wrist and hand, the experimental group outranked the control group significantly only in the joints that were directly involved in the robot-aided therapy. Furthermore, the time history of the scores suggests that the control group did not improve after six weeks from the stroke onset, while seven patients in the experimental group continued to improve up to eight weeks poststroke [36]. At the same time, the rehabilitation experience achieved its stated goal, with both the experimental and control group having a similar increase in the FIM score during their hospital stay ($p = 0.51$, one-tail t -test). We believe that this may be due to 1) the nonspecific nature of the FIM score, which broadly assesses overall functional recovery and 2) the fact that both groups had the same standard therapeutical experience aiming at functional adaptation and compensatory techniques.

Examples of circles drawn by one of these patients are shown in Fig. 5. The left plot of each pair shows a plan view of the patient's hand movement. The right plot shows the movement's speed. This example covers a whole spectrum of details encountered with patients involved in this trial. The circle traces suggest an initial kinematic planning indicated by the conspicuous displacement segments recognizable by the "straight" line segments and changes in movement direction. The last plot of the circle trace (week 11) suggests connectivity between displacement segments. Similarly, the corresponding speed profiles on the right column cover a wide spectrum. Initially, there is minimal connectivity between segments, and the speed of the movement drops to a minimum. Note the shape of almost isolated speed segments (symmetric and minimum-jerk bell-shape). These disconnected speed segments apparently evolved to coalesced speed submovements. Fig. 6 shows on the left column the peaks in curvature and on the right column the movement speed and the reconstructed profile. The peaks counted to determine the maximum number of basis (Cn) are indicated by a circle. Note that peaks occurring at the edge of the interval and below 5% of the maximum curvature peak are not considered. Furthermore, due to the common speed reversal at the end of the movement, some of the peaks occurring close to the trailing edge are included and others not. Fig. 7 shows again the movement speed and the reconstructed profile. The subject was capable of performing a task that involved both joints (shoulder and elbow). The time to perform the task apparently is decreasing with training, as indicated by the movement duration in the figure's right column. Furthermore, note in the same column that the degree of overlap between segments increases with training. These successive observations of the patient's speed profile suggest that the movement was accomplished using a sequence of segments and as training and recovery progressed, these segments appeared to become more overlapped or blended and began to resemble the profile of an unimpaired subject [see Fig. 3(a)], as indicated by the relation between the sum of the segments duration and the movement duration (see Fig. 7, right column). We therefore postulate that the process of poststroke motor recovery may be characterized and rigorously quantified by the pattern of timing and blending of these apparent segments. Moreover, we speculate that this recovery process might conform to models of motor learning, in which the task may initially be performed using a sequence of overlapping segments, which progressively "blend" as motor learning proceeds.

IV. CONCLUSION

Mostly because of the small sample size, these results should be interpreted with caution. Nevertheless, they are encouraging. In summary, our results suggest the following:

- robot-aided therapy had no adverse effect and was well tolerated by the patients;
- nurture positively influenced nature, i.e., exercise therapy influenced motor recovery;
- the combination of robotics and automation technology with concepts from motor control and neuroscience may lead to better tools to evaluate and understand the mechanism of recovery.

To address the limitation of the small sample size and to confirm the pilot trial's encouraging results, we are engaged in a follow-up clinical trial with a larger pool of 60 stroke patients, but already it is not far fetched to suggest that robot technology may be a promising new tool for neurological rehabilitation. We further speculate that the richness of robot-aided information might allow a quantitative insight about what patient population may benefit from exercise therapy, e.g., based on lesion, location, and size, and permit the appropriate exercise routine to be tailored to the patient, e.g., emphasizing accuracy or speed of movement, strength or endurance. Finally, robot-aided neuro-rehabilitation might contribute to cost savings as depicted in Fig. 8 and Fig. 9 by allowing a clinician to work with more than a patient at a time, and by permitting meaningful self-therapy at home. Given the present emphasis on cost containment, this may be particularly important.

ACKNOWLEDGMENT

The authors would like to especially thank L. Edelstein (OTR) of Burke Rehabilitation Hospital.

This work was supported in part by the NSF under Grant 8914032-BCS, the National Parkinsons Disease Foundation, and the Burke Institute for Medical Research.

REFERENCES

1. Butefisch C, Hummelsheim H, Denzler P, Mauritz KH. Repetitive training of isolated movements improves the outcome of motor rehabilitation of the centrally paretic hand. *J. Neurologic. Sci* 1995;vol. 130:59–68.
2. Taub E, Miller NE, Novack TA. Technique to improve chronic motor deficit after stroke. *Arch. Phys. Med. Rehab* 1993;vol. 74:347–354.
3. Wolf SL, Lecraw DE, Barton LA, Jann BB. Forced use of hemiplegic upper extremities to reverse the effect of learned nonuse among chronic stroke and head-injured patients. *Exper. Neurol* 1989;vol. 104 (no 2):125–132. [PubMed: 2707361]
4. Suderland A, Tinson DJ, Bradley EL, Fletcher D, Langton Hewer R, Wade DT. Enhanced physical therapy improves recovery of arm function after stroke. A randomized controlled trial. *J. Neurology. Neurosurg. Psych* 1992;vol. 55:530–535.
5. Dam M, Tonin P, Casson S, Ermani M, Pizzolato G, Iaia V, Battistin L. The effects of long-term rehabilitation therapy on poststroke hemiplegic patients. *Stroke* 1993;vol. 24(no 8):1186–1191. [PubMed: 8342195]
6. Wolf SL, Binder-Macleod SA. Electromyographic biofeedback applications to the hemiplegic patient: Changes in upper extremity neuromuscular and functional status. *Physic. Therapy* 1983;vol. 63:1393.
7. Smith LE. Restoration of volitional limb movement of hemiplegics following patterned functional electrical stimulations. *Percep. Motor Skills* 1990;vol. 71:851–861.
8. Logigian MK, Samuel MA, Falconer JF. Clinical exercise trial for stroke patients. *Arch. Phys. Med. Rehab* 1983;vol. 64:364–367.
9. Dickstein R, Hocherman S, Pillar T, Shaham R. Stroke rehabilitation—Three exercise therapy approaches. *Physic. Therapy* 1986;vol. 66:1233–1238.
10. Chollet F, DiPiero V, Wise RJS, Brooks DJ, Dolan RJ, Frackowiak RSJ. The functional anatomy of motor recovery after stroke in humans: A study with positron emission tomography. *Ann. Neurol* 1991 Jan;vol. 29(no 1):63–71. [PubMed: 1996881]
11. Fisher CM. Concerning the mechanism of recovery in stroke hemiplegia. *Canadian J. Neurol. Sci* 1992;vol. 19:57–63.
12. Jacobs KM, Konoghue JP. Reshaping the cortical motor map by unmasking latent intracortical connections. *Sci* 1991;vol. 251:944–947.
13. Merzenich MM, Nelson RJ, Stryker MP, Cynader MS, Schoppmann A, Zook JM. Somatosensory cortical map changes following digit amputation in adult monkeys. *J. Comparative Neurol* 1984;vol. 224:591–605.

14. Pons TP, Garraghty PE, Mishkin M. Lesion-induced plasticity in the second somatosensory cortex of adult macaques. *Proc. Nat. Academy Sci* 1988;vol. 85:5279–5281.
15. Kaas JH, Krubitzer LA, Chino YM. Reorganization of retinotopic cortical maps in adult mammals after lesions of the retina. *Sci* 1990;vol. 248:229–231.
16. King AJ, Moore DR. Plasticity of auditory maps in the brain. *Trends Neurosci* 1991;vol. 14:21–27.
17. Nudo RJ, Wise BM, SiFuentes F, Milliken GW. Neural substrates for the effects of rehabilitative training on motor recovery after ischemic infarct. *Sci* 1996;vol. 272:1791–1794.
18. Aisen ML, Krebs HI, McDowell F, Hogan N, Volpe BT. The effect of robot assisted therapy and rehabilitative training on motor recovery following stroke. *Arch. Neurol* 1997 Apr;vol. 54:443–446. [PubMed: 9109746]
19. Hogan, N.; Krebs, HI.; Sharon, A.; Charnnarong, J., inventors. Interactive robotic therapist. U.S. Patent. #5 466 213. 1995.
20. Hogan N. Impedance control: An approach to manipulation: Part I, Part II, Part III. *J. Dynam. Syst., Measurement, Contr.—Trans. ASME* 1985;vol. 107:1–24.
21. Hogan N. On the stability of manipulators performing contact tasks. *IEEE J. Robot. Automat* 1988;vol. 4:677–686.
22. Colgate JE, Hogan N. Robust control of dynamically interacting systems. *Int. J. Contr* 1988;vol. 48 (no 1):65–88.
23. Trombly, CA. *Occupational Therapy for Physical Dysfunction*. Baltimore, MD: Williams and Wilkins; 1995.
24. Fugl-Meyer AR, Jaasco L, Leyman L, Olsson S, Steglind S. The post-stroke hemiplegic patient. *Scand. J. Rehab. Med* 1975;vol. 7:13–31.
25. Aisen ML, Sevilla D, Gibson G, Kutt H, Blau A, Edelstein L, Hatch J, Blass J. 3,4-diaminopyridine as a treatment for amyotrophic lateral sclerosis. *J. Neurologic. Sci* 1995;vol. 129:21–24.
26. Woodworth, RS. *The Psychologic. Rev. Vol. vol. III*. The Macmillan Company; 1899 Jul. Accuracy of voluntary movement.
27. Crossman ERFW, Goodeve J. Feedback control of hand-movement and Fitts' law. *Quart. J. Exper. Psychol* 1983;vol. 35A:251–278.
28. Morasso P, Mussa-Ivaldi FA. Trajectory formation and handwriting: A computational model. *Biologic. Cybern* 1982;vol. 45:131–142.
29. Jagacinski RJ, Hartzell EJ, Ward S, Bishop K. Fitts' law as a function of system dynamics and target uncertainty. *J. Motor Behavior* 1978;vol. 10:123–131.
30. Jagacinski RJ, Repperger DW, Moran MS, Ward SL, Glass B. Fitts' law and the microstructure of rapid discrete movements. *J. Exper. Psychol.: Human Perception and Performance* 1980;vol. 6(no 2):309–320.
31. Krebs, HI. Ph.D. dissertation. Massachusetts Inst. Technol.; 1997 Feb. Robot-aided neuro-rehabilitation and functional imaging.
32. Krebs HI, Hogan N, Aisen ML, Volpe BT. Pilot clinical trial of a robot-aided neuro-rehabilitation workstation with stroke patients. *Proc. SPIE—Telemanipulator Technol* 1996 Nov;vol. 2901:13–21.
33. Viviani P, Terzuolo C. Trajectory determines movement dynamics. *Neurosci* 1982;vol. 7:431–437.
34. Poggio T, Girosi F. Regularization algorithm for learning that are equivalent to multilayer networks. *Sci* 1990 Feb 23;vol. 247:978–982.
35. Dijkers M, deBear P, Erlandson RF, Kristy K, Geer D, Nichols A. Patient and staff acceptance of robotic technology in occupational therapy: A pilot study. *J. Rehab. Res. Dev* 1991;vol. 35(no 2): 33–44.
36. Reinkensmeyer, DJ.; Hogan, N.; Krebs, HI.; Lehman, SL.; Lum, PS. Rehabilitators, robots, and guides: New tools for neurological rehabilitation. In: Winters, JM.; Crago, PE., editors. *Biomechan. Neural Contr. Movement*. New York: Springer-Verlag; 1998. to be published.

Biography



Hermano Igo Krebs (M'92) received the electrician degree in 1976 from Escola Tecnica Federal de Sao Paulo, Brazil, the B.S. and M.S. degrees in naval engineering (option electrical) from University of Sao Paulo, Brazil, in 1980 and 1987, respectively, with the M.S. thesis "A Study of an Integrated Autopilot for Ships." He received another M.S. degree in ocean engineering from Yokohama National University, Japan, in 1989, with the thesis "On an Optimal Linear Quadratic Autopilot for Minimum Fuel Consumption," and the Ph.D. degree in ocean engineering from the Massachusetts Institute of Technology (MIT), Cambridge, in 1997, with the thesis "Robot-Aided Neuro-Rehabilitation and Functional Imaging."

From 1977 to 1978, he taught electrical design at Escola Tecnica Federal de Sao Paulo. From 1978 to 1979, he worked at University of Sao Paulo in a project aiming at the identification of hydrodynamic coefficients during ship maneuvers. From 1980 to 1986, he was a surveyor of ships, offshore platforms, and container cranes at the American Bureau of Shipping, Sao Paulo office, Brazil. In 1989, he was a Visiting Researcher at Sumitomo Heavy Industries, Hiratsuka Laboratories, Japan. From 1993 to 1996, he worked at Casper, Phillips & Associates in containercranes and control systems. During the first part of 1997, he was a Postdoctoral Associate at MIT, and since the later part of 1997, he is a research scientist at MIT in the Mechanical Engineering Department, Newman Laboratory for Biomechanics and Human Rehabilitation. His research interests are in the areas of dynamic systems modeling and control, robotics, human-machine interactions, neuromotor control, robot-aided functional imaging, and robot-aided neurorehabilitation.

Neville Hogan was born in Ireland and received the Diploma in engineering (with distinction) from the College of Technology in Dublin, Ireland, in 1970. He received the M.S. degree in mechanical engineering in 1973, the Mechanical Engineer degree in 1976, and the Ph.D. degree in mechanical engineering in 1977, all from the Massachusetts Institute of Technology (MIT), Cambridge.

He worked in industry as a Product Development and Design Engineer and joined the Faculty of the Massachusetts Institute of Technology in 1979. He is currently Professor of Mechanical Engineering and Brain and Cognitive Sciences, and Director of the Newman Laboratory for Biomechanics and Human Rehabilitation. His research interests include robotics, biomechanics, and neural control of movement, emphasizing contact tasks and tool use. He proposed impedance control as a method for controlling motion and dynamic interaction in natural and artificial systems. Applications include arm amputation prostheses, robotics, telerobotics, haptic virtual environment and human performance enhancement technologies. His teaching responsibilities are in the areas of physical system dynamics and control, machine design, and quantitative physiology.

Mindy L. Aisen received the B.S. degree in mechanical engineering from the Massachusetts Institute of Technology (MIT), Cambridge, in 1976 and the M.D. degree from Columbia University College of Physicians and Surgeons, NY, in 1980.

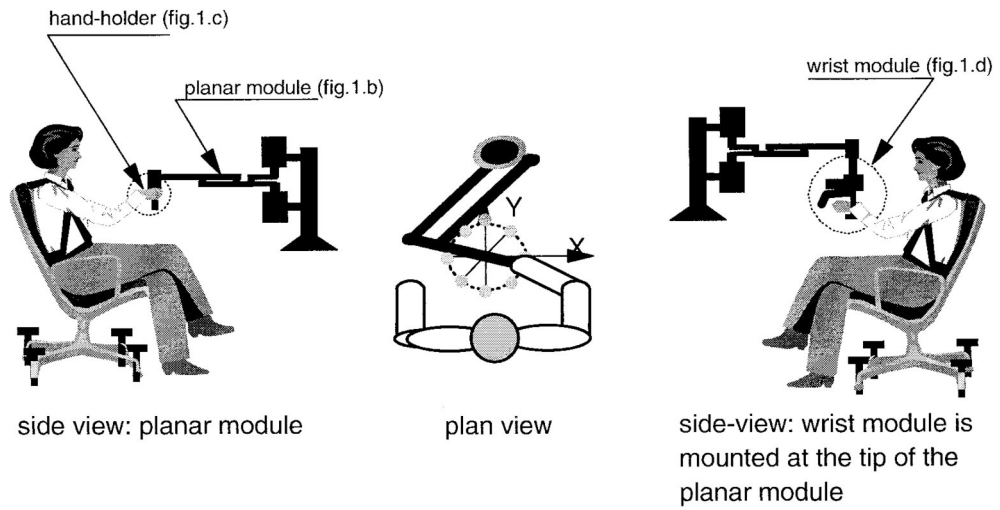
She trained in medicine and neurology at the Mount Sinai Hospital of Cleveland and at The New York Hospital-Cornell Medical Center. After training, she joined the hospital and Faculty of Neurology at The Albert Einstein College of Medicine from 1984 to 1987. In 1987, she joined The New York Hospital, and became the Director of the Spinal Cord Injury Service, The Burke Rehabilitation Hospital, White Plains, NY. She became an Associate Professor of Clinical Neurology at Cornell University Medical College, White Plains, NY, in 1994, and an Adjunct Professor of Physical Medicine and Rehabilitation at Cornell University Medical College in 1998.

Dr. Aisen is a member of the Board of Directors of the American Society of Neurorehabilitation, Chair of the Research Committee of the American Society of Neurologic Rehabilitation, Assistant Editor of the *Journal of Neurologic Rehabilitation*, member of the Scientific Advisory Board of Paralyzed Veterans of America, and member of the grant review panel of the National Multiple Sclerosis Society.

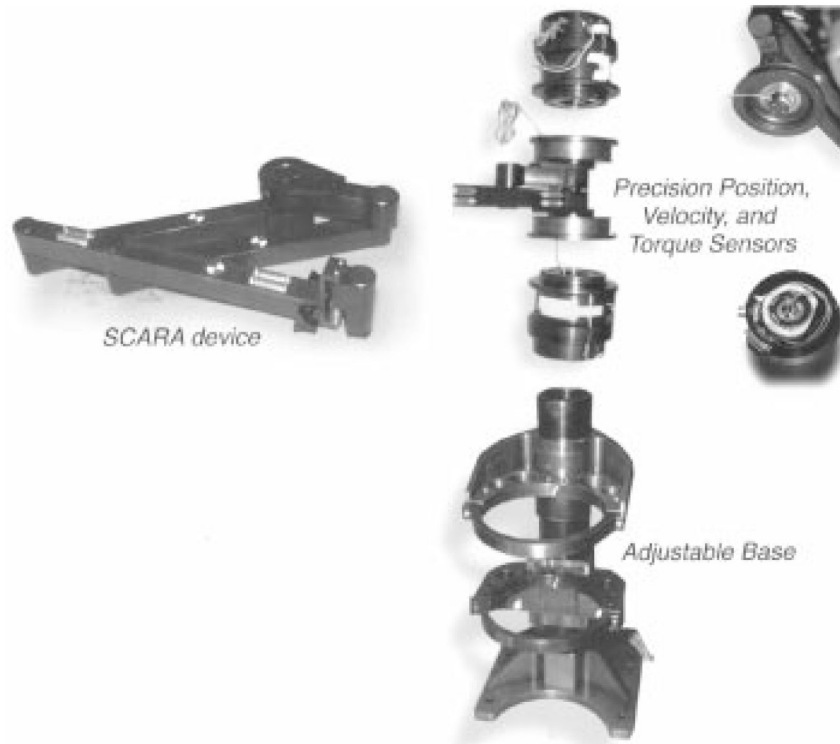
Bruce T. Volpe received the B.S. degree in 1969 and the M.D. degree in 1973 from Yale University, New Haven, CT.

He trained in medicine and neurology at University of Chicago, IL, and College of Physicians and Surgeons, Columbia University, NY, and Cornell University Medical College, White

Plains, NY. After training, he joined the Faculty of Neurology and Neuroscience at Cornell Medical College, where he is now a Professor. He has been a member of the Burke Medical Research Institute, where his interests include the mechanisms of delayed neuronal death and the mechanisms of motor recovery.



(a)



(b)

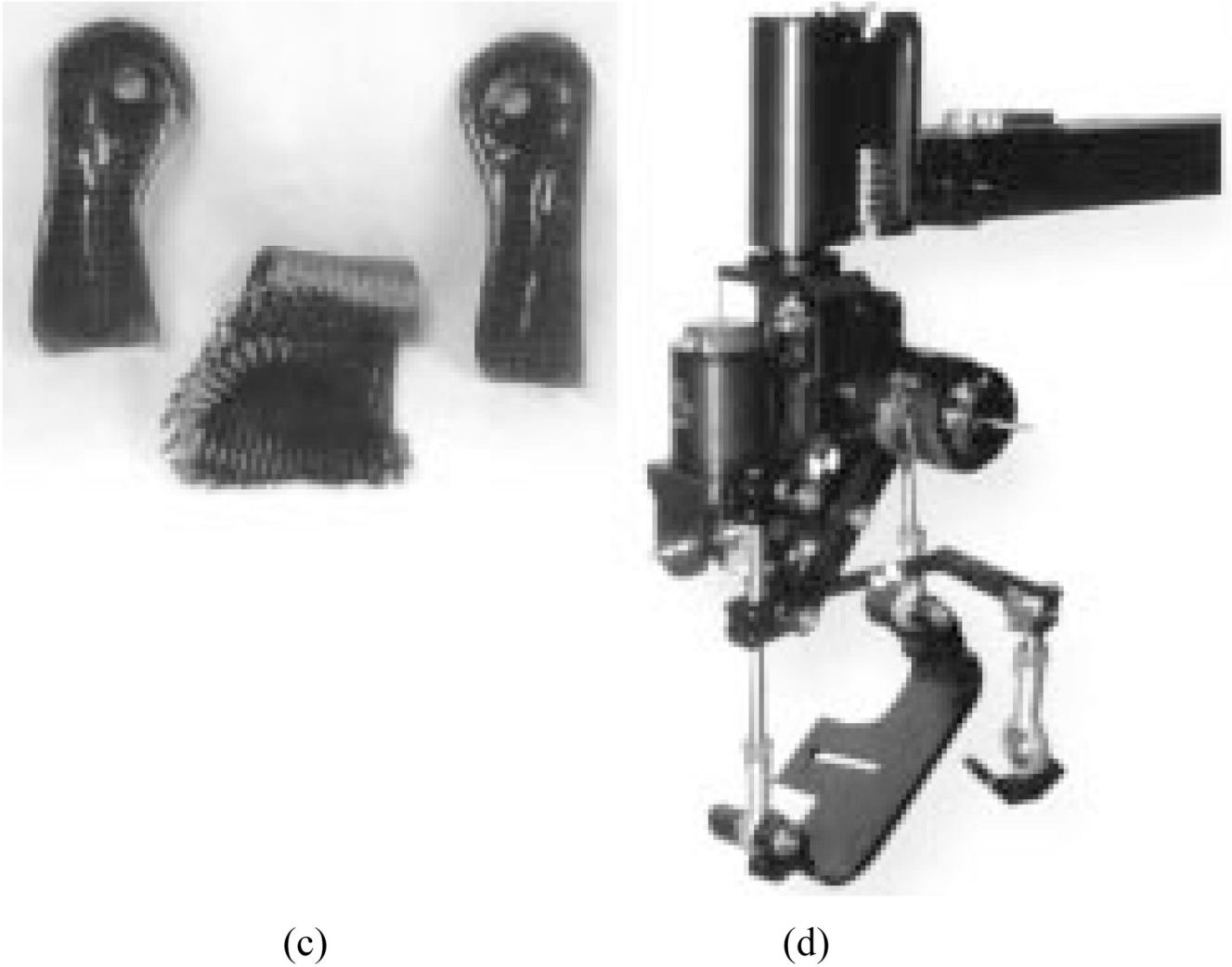


Fig. 1.

(a) MIT-MANUS: Assembly sketch. The sketch shows a patient during the robot-aided neurorehabilitation session. Patient sat facing the robot and was required to move the robot end-effector according to the game's goals. If the patient could not perform the task in response to a visual and auditory cue, the robot assisted and guided the patient's hand. The left side sketch shows a patient working only with the planar module, a direct-drive five bar-linkage SCARA mechanism which provides two translational degrees of freedom for elbow and forearm motion [see Fig. 1(b)]. A custom-made hand-holder connects the patient's impaired limb to the robot end-effector [see Fig. 1(c)]. The right side sketch shows a patient working with the planar module and the wrist module [see Fig. 1(d)], which is mounted on the end of the planar module and provides three degrees of freedom for wrist motion. (b) MIT-MANUS: Planar module (not in scale). (c) MIT-MANUS: Custom-made hand-holders for the planar module (not in scale). (d) MIT-MANUS: Wrist module (not in scale).

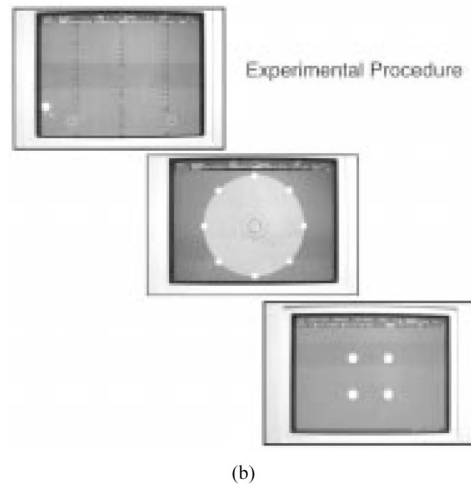
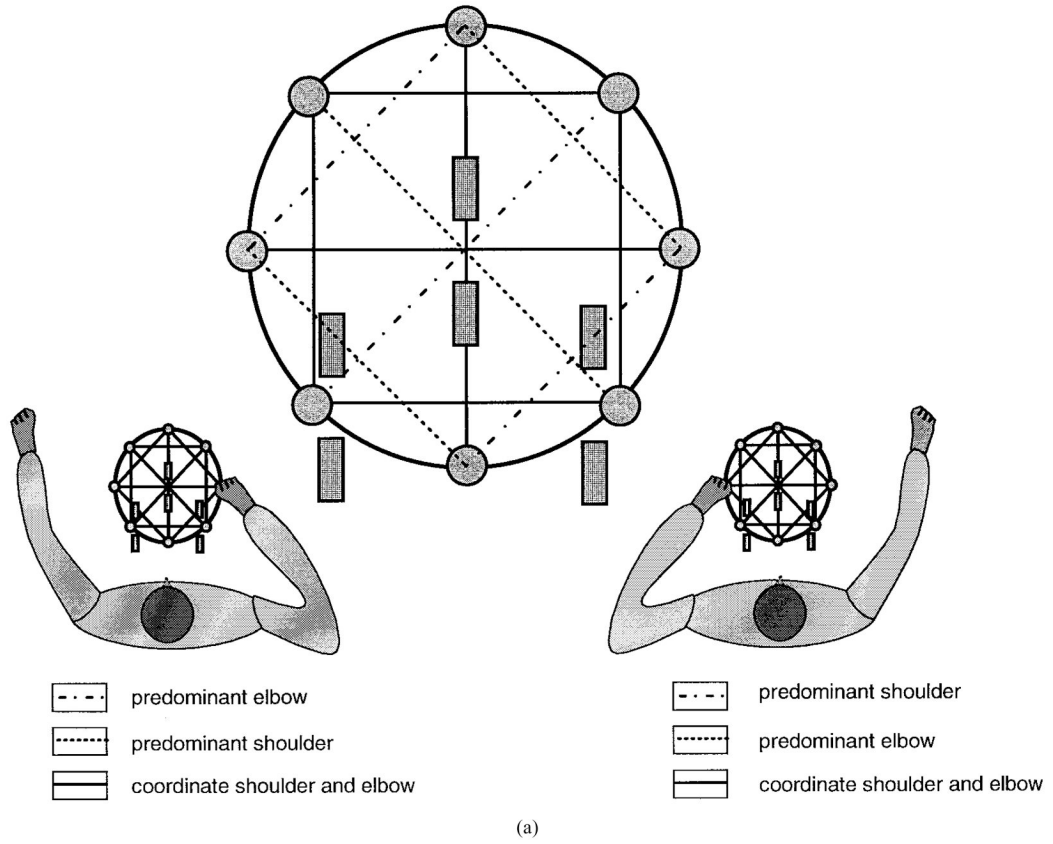


Fig. 2. (a) Video-games: Elbow and shoulder exercises. Targets were arranged so that diagonal paths required predominantly elbow or shoulder motions while vertical, horizontal or curved paths required coordination of both. (b) Video-games: Visual displays. The games included drawing circles, stars, squares, diamonds, and navigating through windows.

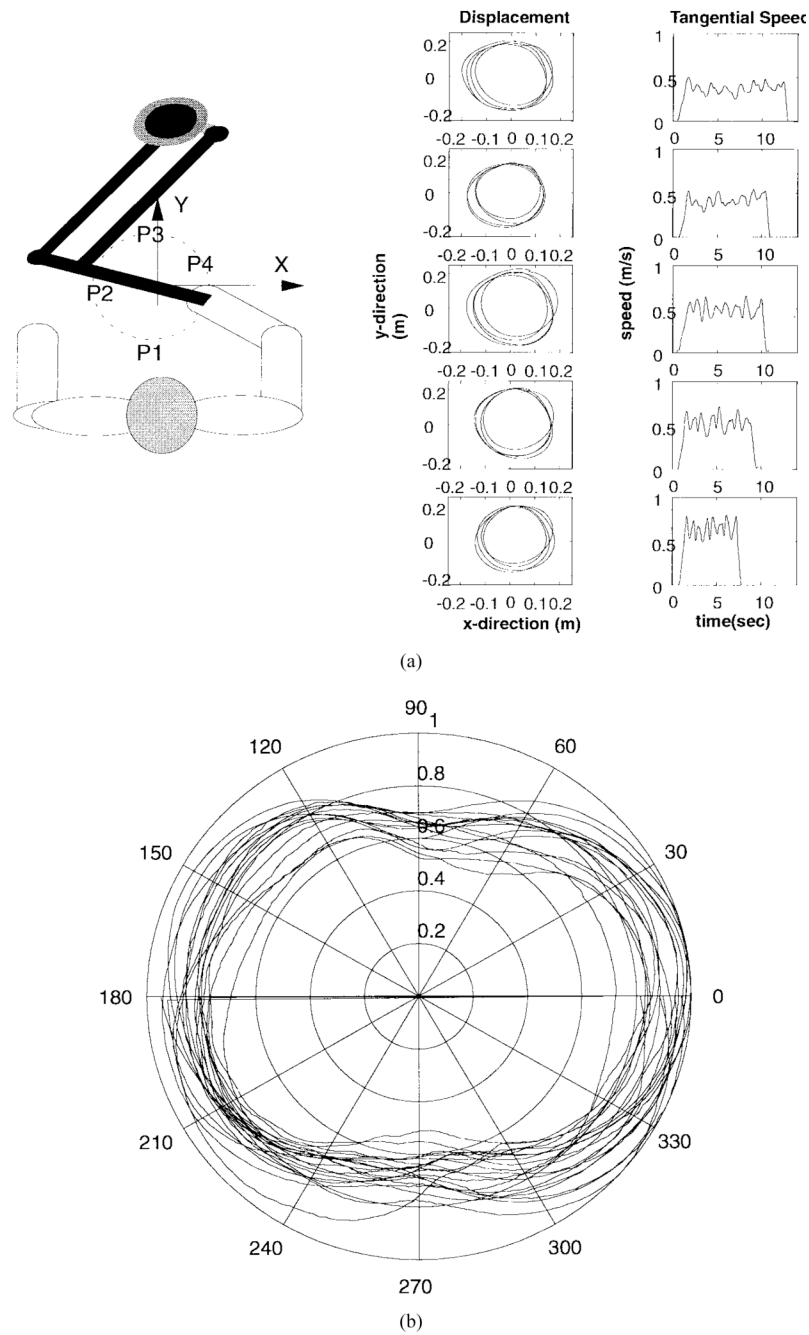


Fig. 3. (a) Drawing four circles at constant speed. Subject grasped the robot handle with the palm and was instructed to draw circles at constant speed. His hand was within view, but no explicit feedback was provided. The trial was repeated at faster speeds until the subject considered himself unable to maintain constant speed. The left column shows the circle traces and the right column shows the speed profiles at different target constant speeds. Note the oscillatory characteristic of the speed in all trials. (b) Polar plots of four circles drawn at different target constant speeds. The plot shows a composite of all trials of (a). Speed was normalized and the initial accelerating and decelerating phases were omitted. Note the kinematic (not temporal) characteristic of plot.

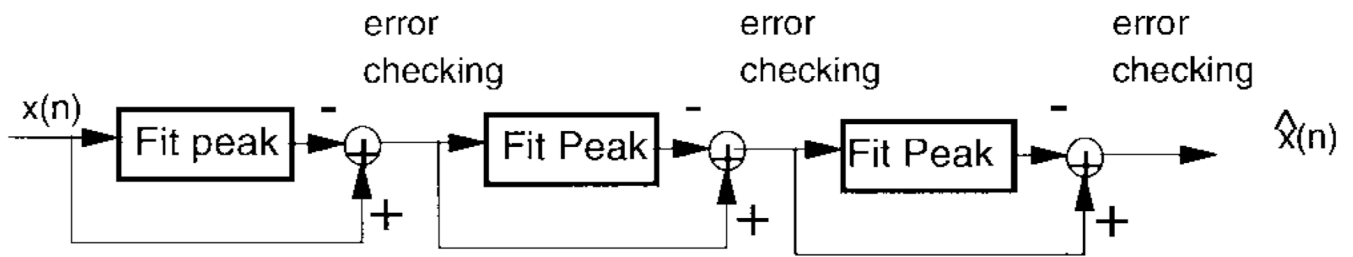


Fig. 4. Irregular sampling radial basis function (ISRBF). The figure illustrates the ISRBF approach. It resembles a pyramidal filter, in which a “mother” shape is fitted to the function’s largest peak. If the remainder is above an error bound, and the number of bases does not surpass the upperbound limit obtained from the curvature analysis, the process is reiterated.

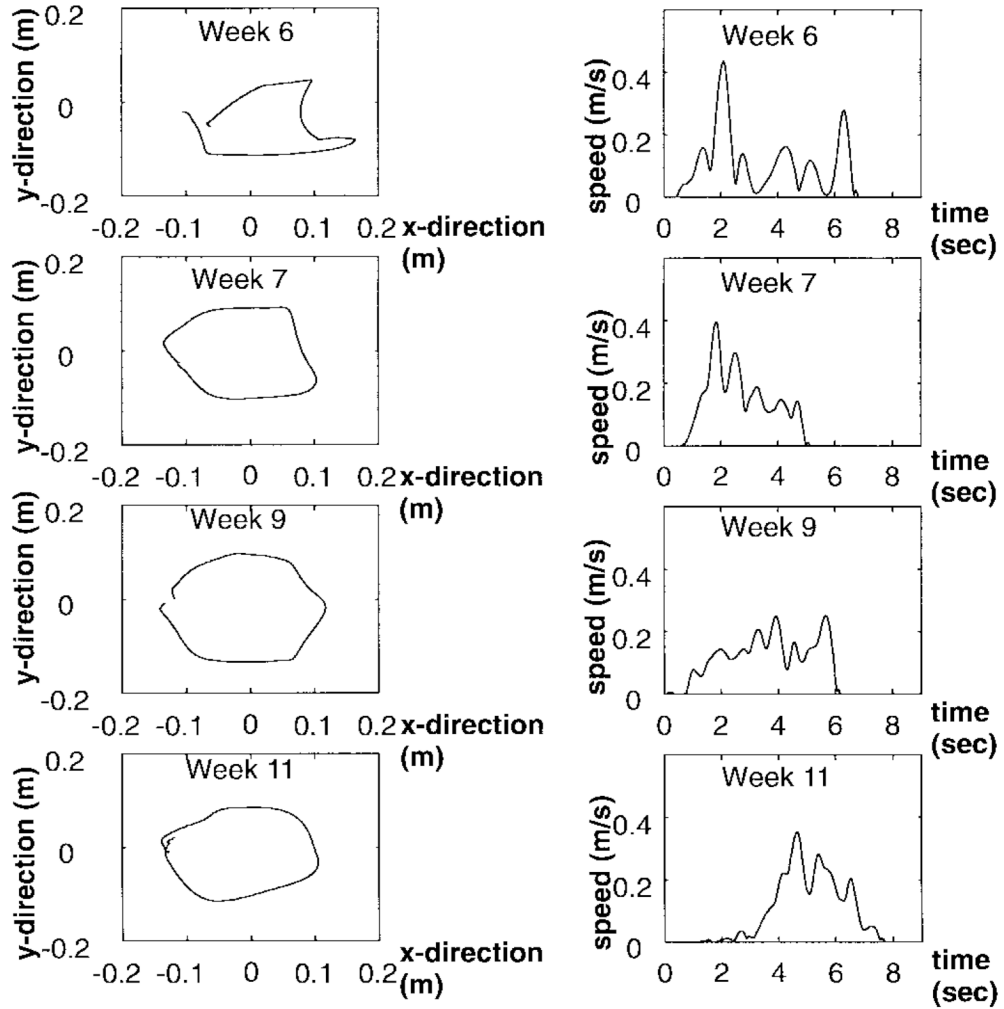
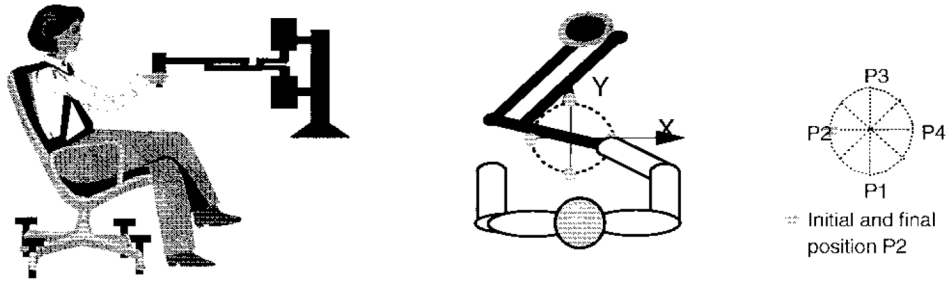


Fig. 5. Patient (A) drawing clockwise circles starting and ending at position P2 (9 o'clock). The patient was wearing a hand-holder that connects his/her palm to the robot end-effector and the elbow was supported against gravity. The patient was instructed to draw a smooth circle. The hand was within view, but no explicit feedback was provided.

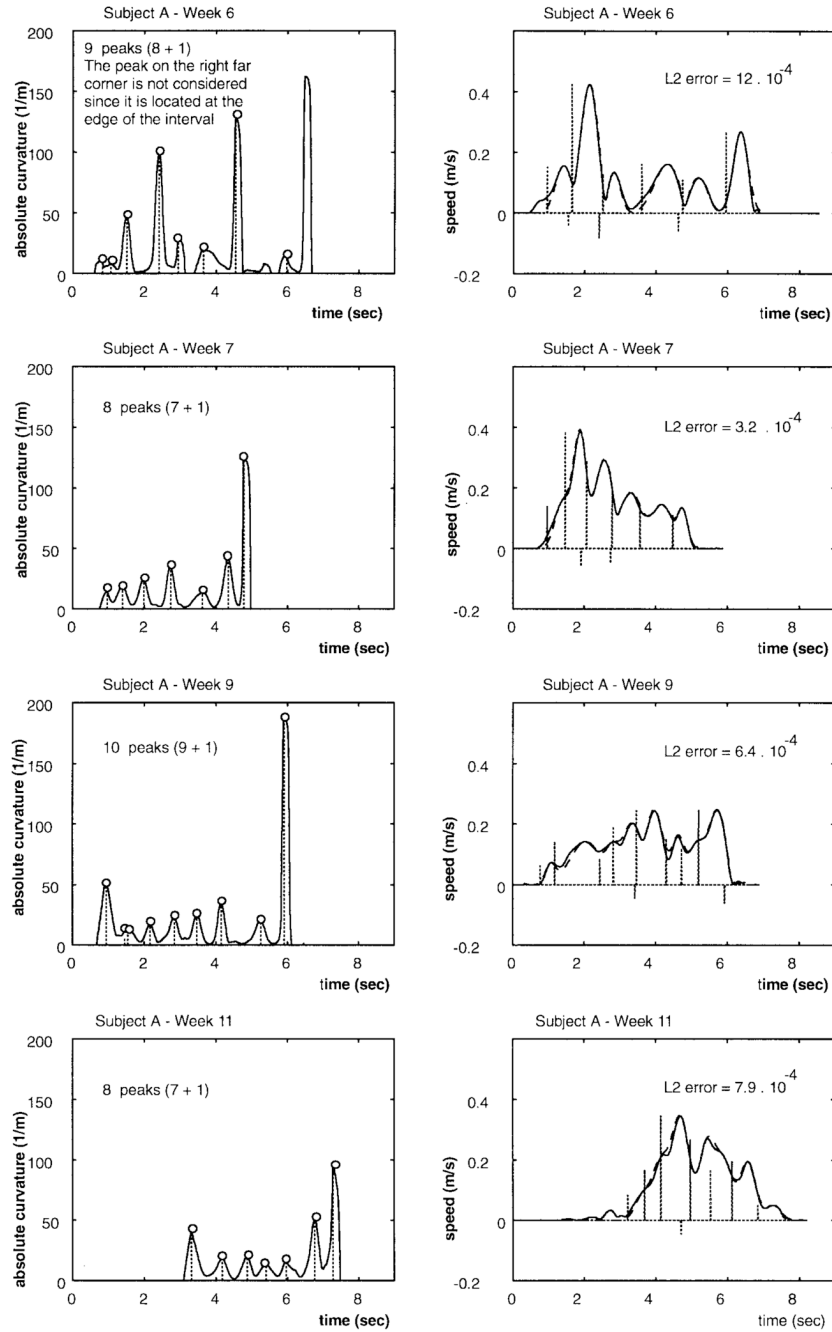


Fig. 6. Application of the irregular sampling radial basis function algorithm (ISRBF) to the circles of Fig. 5. In the first step (left column), the maximum number of bases (C_n) is obtained from the peaks in curvature. Peaks at the edge of the interval and below 5% of maximum peak are not considered, but an extra peak is added to C_n to account for the edges. The “mother” shape is fitted to the symmetric regions around the peaks. The process stops if the error of the approximation is below a predetermined threshold or the process uses C_n bases. The resulting approximation is shown in the right column.

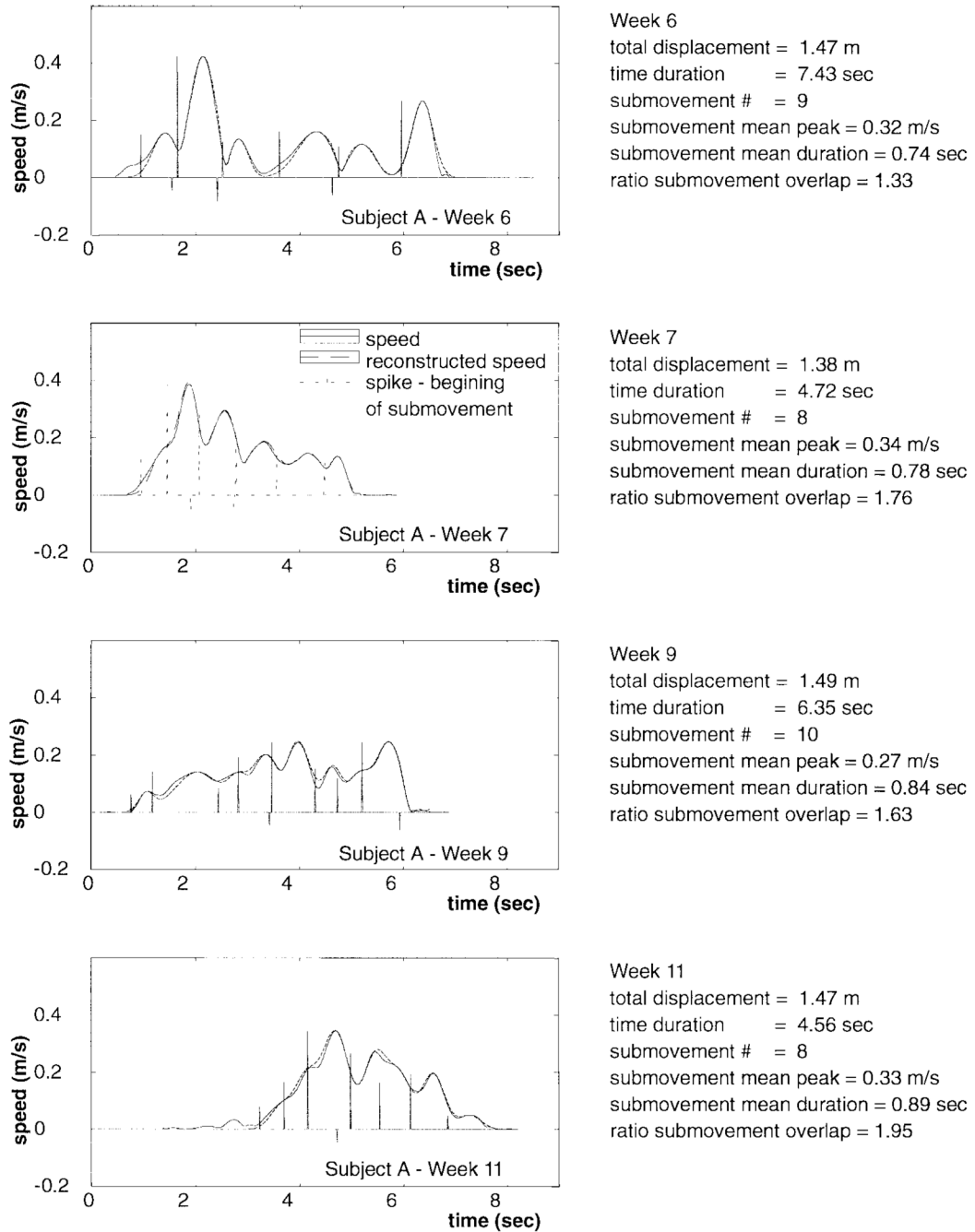


Fig. 7. Apparent changes in movement composition with recovery. The ISRBF algorithm suggests that movement duration is decreasing (see right column: time duration), apparent segment duration is increasing (see right column: submovement mean duration), and the degree of overlap of submovements may be increasing, indicating blending (see right column: ratio of submovement overlap). There is no apparent trend for the path length, number of submovements, or mean peak speed.

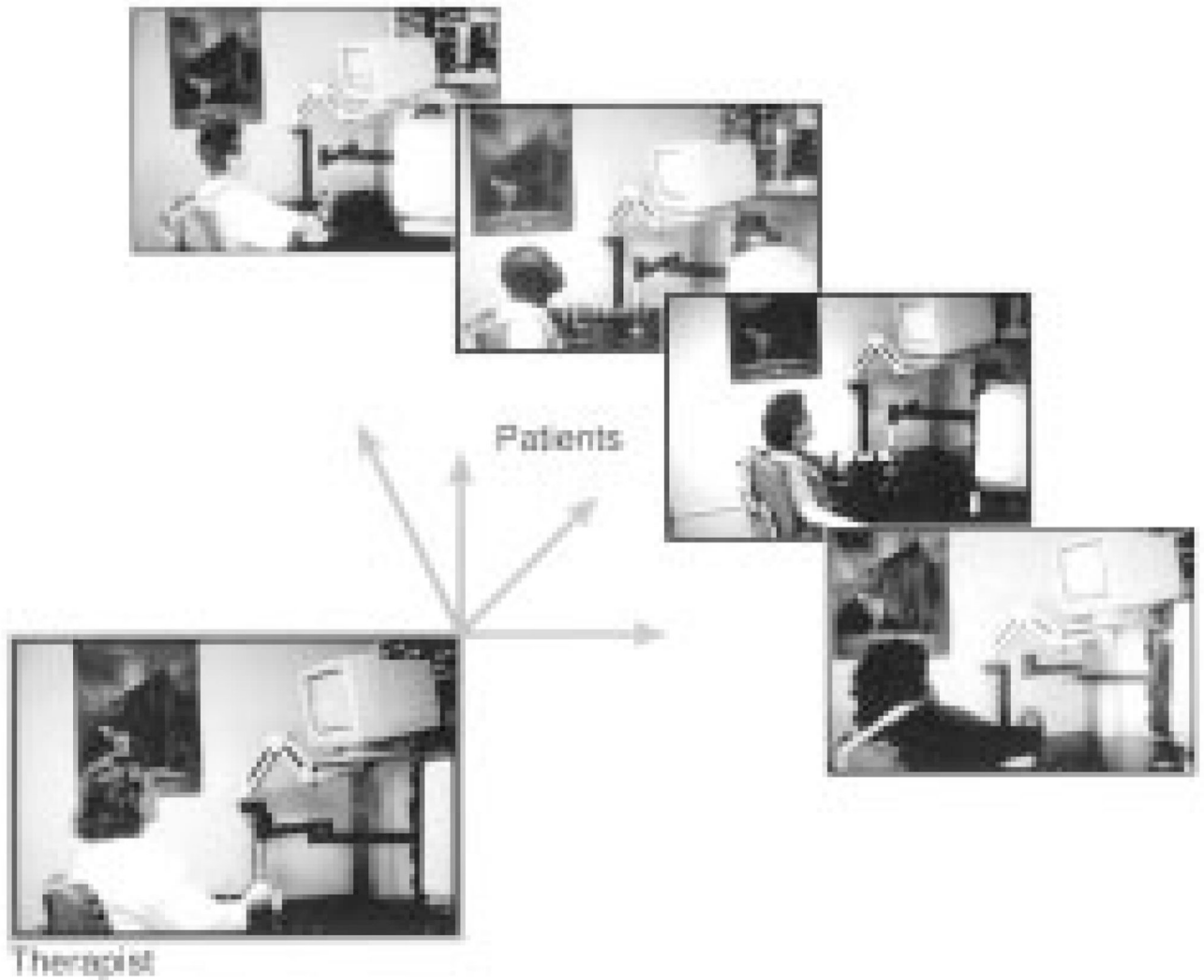


Fig. 8. Robot-aided neurorehabilitation: Classroom or group session. This figure illustrates the potential for cost-containment by allowing a clinician to work with more than one patient at a time.

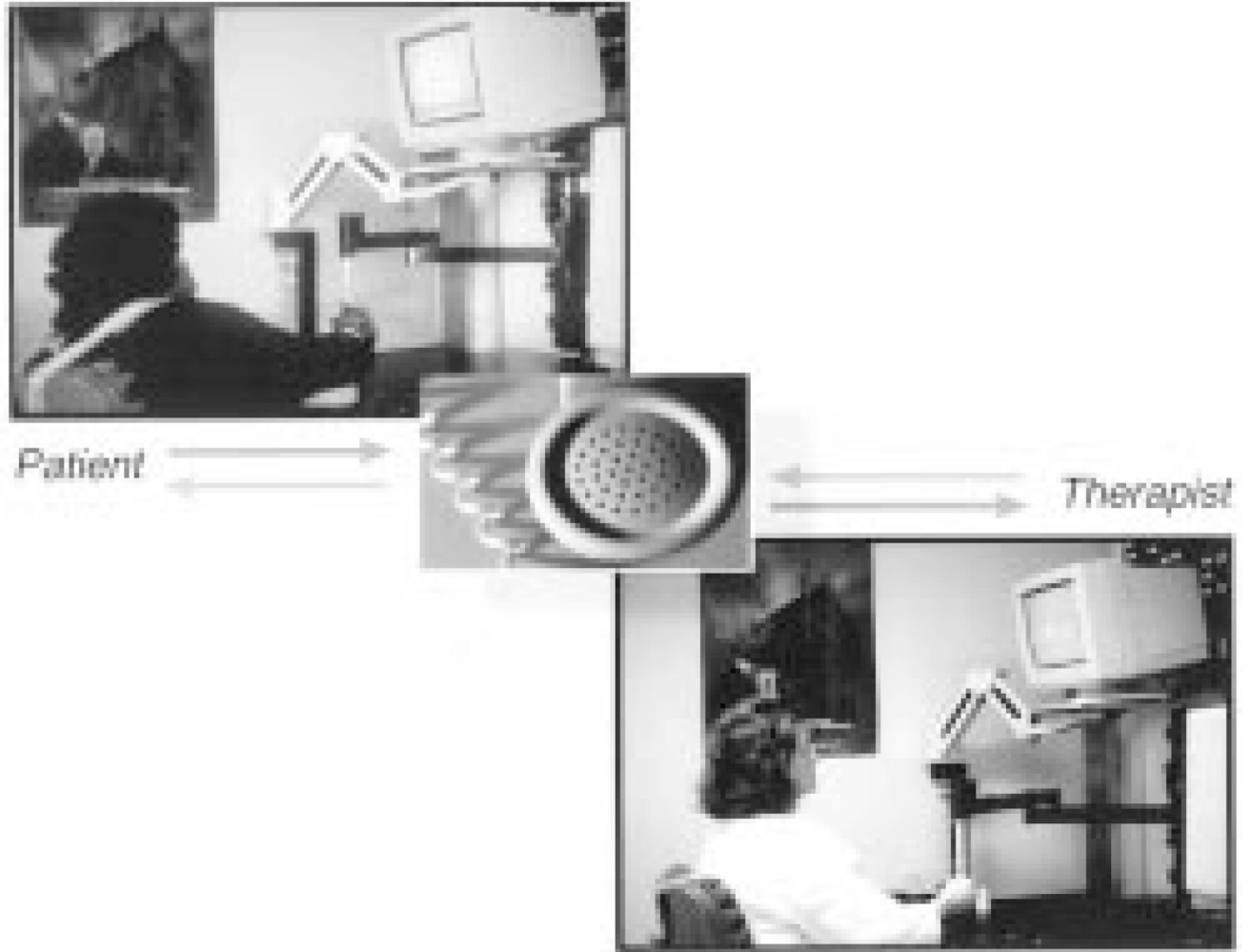


Fig. 9. Robot-aided neurorehabilitation: Self-care therapy at home. The clinician telementors an out-patient via a bilateral link between the robot in the home and the robot in the clinic.

TABLE I
Patients' Tolerance for the Procedure

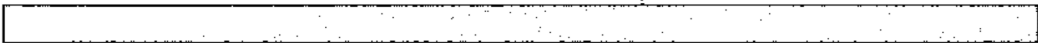
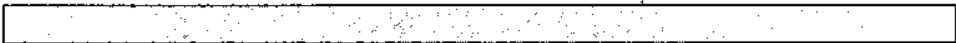
	Disagree				Agree				Mean Value
	Strongly 0	Moderately 1	Somewhat 2	Little 3	Little 4	Somewhat 5	Moderately 6	Strongly 7	
1. Comfortable with the robot therapy									5.92
2. Enjoyed doing therapy with the robot									5.71
3. Believe the robot therapy sessions were beneficial									5.67
4. Working with the robot helps in ways that nobody else can									4.82
5. Would like to perform more therapy with the robot									5.48
6. Would rather work with the robot than a therapist									2.58

TABLE II

Change During Acute Rehabilitation: Mean, Standard Deviation, P-value for the Trial's Groups with Standard Assessment Scales—(*) Indicates Data for Nine Patients

Group	Experimental (10 patients)	Control (10 patients)	One-Tail t-test (significant $p < 0.05$)
Change FIM (range 126 pts)	25.6±7.2	25.7 ±12.2	0.51
Change F-M -- UE subscore (range 66 pts)	14.1 ± 9.7	9.9±11.2	0.19
Change MP (range 20 pts)	3.9±2.9	2.3± 2.4	0.10
Change MSS -- shoulder/elbow (range 40 pts)	9.4±5.9 (*)	0.8± 3.8	0.00065
Change MSS -- wrist (range 6 pts)	0.9±1.5(*)	0.5± 1.5	0.29
Change MSS -- hand (range 36 pts)	4.6±6.4(*)	3.5± 6.3	0.36